Uluslararası İleri Doğa Bilimleri ve Mühendislik Araştırmaları Dergisi
Sayı 8, S. 1-6, 10, 2024

Araştırma Makalesi

IJANSER
https://as-proceeding.com/index.php/ijanser
ISSN:2980-0811

International Journal of Advanced Natural Sciences and Engineering Researches
Volume 8, pp. 1-6, 10, 2024

Research Article

High-Temperature Effect on Mechanical Properties of GGBS-Based Geopolymer Composites Having Bauxite Residue

Shahir Ahmad Safi[*1], Ali Raza [1], Mujib Ul Rahman Rahmani[1] and Abdellatif Selmi [2]

[1] *Department of Civil Engineering, University of Engineering and Technology Taxila, 47050, Pakistan*
[2] *Prince Sattam Bin Abdulaziz University, College of Engineering, Department of Civil Engineering, Alkharj, 11942, Saudi Arabia*

[*]*(shahirahmad229@gmail.com)*

(Received: 03 November 2024, Accepted: 16 November 2024)

(3rd International Conference on Contemporary Academic Research ICCAR 2024, 10-11 November 2024)

ATIF/REFERENCE: Safi, S. A., Raza, A., Rahmani, M. U. R. & Selmi, A. (2024). High-Temperature Effect on Mechanical Properties of GGBS-Based Geopolymer Composites Having Bauxite Residue, *International Journal of Advanced Natural Sciences and Engineering Researches*, 8(10), 1-6.

Abstract – This study investigated the influence of partially replacing calcined bauxite residue (BR) with ground granulated blast furnace slag (GGBS) and calcium sulfate dihydrate (CSD) in geopolymer concrete (GC). The test program included tests on the mechanical properties of these blends, including flexural strength and split tensile strength at ambient and elevated temperatures. All GC blends showed increased flexural and split tensile strengths over time due to ongoing geopolymerization, with mix R40-G45-C15 achieving the highest gains—53.66% and 112.42% higher than mix R70-G15-C15 at 28 days. At elevated temperatures (250°C, 500°C, 750°C), the compressive strength of R40-G45-C15 decreased from 45.27 MPa to 11.41 MPa, while flexural and tensile strengths declined from 6.21 MPa to 2.34 MPa and from 4.57 MPa to 1.99 MPa, respectively.

Keywords – Geopolymer; calcined bauxite residue; mechanical properties; tensile strength, flexural strength, elevated temperatures

I. INTRODUCTION

Geopolymers are defined by alkali-activated aluminosilicate-rich units forming a semi-crystalline, three-dimensional network. Unlike traditional Portland cement, they do not require calcination, resulting in reduced CO2 emissions and lower use of natural resources, alongside the cost-effective integration of industrial waste [1-5]. Compared to Portland cement, geopolymers exhibit enhanced durability in corrosive conditions such as high temperatures and sewage [6, 7]; however, large-scale application remains challenging due to the energy-intensive and costly nature of commercial alkali activators, like sodium silicate, which may necessitate specialized pressure or heat drying treatments [8]. Life cycle assessments show that alkali activators such as sodium silicate and potassium/sodium hydroxide are responsible for 74% of greenhouse gas emissions [9].

A review of existing research indicates that while individual use of waste materials (CSD, BR, and GGBS) in GC has been explored, the combined use of calcined BR, CSD, and GGBS for GC synthesis remains under-researched. Thus, a novel approach using calcined BR-, CSD-, and GGBS-based GC with minimal cement has significant potential. In this study, calcination was applied to increase the reactivity of BR in GC production, creating several GC blends with varied amounts of calcined BR, CSD, and GGBS as

aluminosilicate sources. The research focused on evaluating these blends' mechanical properties at both ambient and elevated temperatures.

II. EXPERIMENTAL PROGRAM

i. Materials and Properties

This study incorporates binders in GC, utilizing calcined BR, CSD, and GGBS sourced from diverse origins. Specific gravity values were recorded as 3.15 for BR, 2.42 for CSD, and 2.93 for GGBS. Table 1 presents the X-ray fluorescence (XRF) analysis of the precursor materials. The average particle sizes for BR, CSD, and GGBS were 28.5 μm, 58.9 μm, and 9.5 μm, respectively, with corresponding specific surface areas of 3.5 m^2/g, 1.9 m^2/g, and 0.68 m^2/g. Experimental conditions maintained 99% purity for sodium silicate and NaOH. River sand was used as fine aggregate with a maximum size of 0.75 mm and a specific gravity of 2.68, while coarse aggregate size was limited to 19 mm with a specific gravity of 2.76. To prepare BR, it was first dried at 100 °C in a blast oven, ground in a testing mill for 10 minutes, and mixed with 10% water by weight to create test cakes of 20 cm diameter and 1-2 cm thickness. These cakes were subsequently calcined in a muffle furnace following a designated firing schedule with target temperatures of 500 °C, 600 °C, 700 °C, and 800 °C.

Table 1. XRF results for the chemical compositions of BR, CSD, and GGBS

Compound	BR (%)	CSD (%)	GGBS (%)
Iron oxide (Fe_2O_3)	14.92	1.4	1.56
Alumina (Al_2O_3)	29.74	6.11	18.72
Calcium Oxide (CaO)	12.27	36.84	34.99
Silica (SiO_2)	22.11	7.98	30.59
Sodium oxide (Na_2O)	10.43	0.45	2.06
Sulfur trioxide (SO_3)	0.99	39.74	1.23
Magnesium Oxide (MgO)	1.94	2.14	2.72
Potassium Oxide (K_2O)	3.01	0	2.95
Titania (TiO_2)	0.99	0.27	1.67
Loss on Ignition (LOI)	1.61	3.08	1.53

The calcination process involved raising the activation temperature for 30 minutes, followed by maintaining it for 2 hours. Once calcination was completed, samples were removed from the muffle and promptly cooled to room temperature before being ground for 5 minutes and then sieved using a 0.075 mm mesh. To create mortar specimens, BR and Portland cement were mixed in a 3:7 mass ratio. The activity index was determined by dividing the compressive strength of BR-containing mortar specimens by that of Portland cement specimens after 28 days. Calcination of BR was carried out at temperatures of 500, 600, 700, and 800 °C. The reactivity potential of BR at these various temperatures was assessed through the activity index. As shown in Figure 1, the activity index initially increased with temperature but declined at higher temperatures, peaking at 0.88 at 700 °C—33.33% above the initial BR value of 0.66—before dropping to 0.78 at 800 °C. These findings indicate a threshold temperature for BR calcination, beyond which reactivity potential is not maintained. The results in [10] and [11] support 800 °C as the optimal calcination temperature, although minor discrepancies are linked to the high calcite enrichment in the original BR.

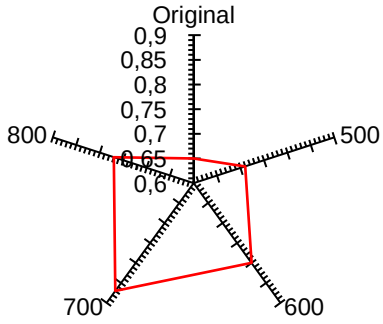

Figure 1. Activity indices of BR at different temperatures.

ii. Fabrication and Testing of Samples

The GC was prepared using 425 kg/m³ of calcined BR, CSD, and GGBS as precursors. The alkali-to-binder ratio was set to 0.47, and a consistent Na2SiO3-to-NaOH ratio of 1.5 was applied across all blends, with a NaOH concentration of 12M. Initially, calcined BR, CSD, GGBS, and aggregates were dry-mixed for 5 minutes, followed by 3 minutes of mixing after adding the alkali solution. The specimens were cast and cured at 80°C for 24 hours; once demolded, they were stored at 25°C for ambient curing. A superplasticizer (SP) amounting to 1% of the binder was included to ensure uniformity in the mix. Testing adhered to ASTM/C143 [12] standards, evaluating mechanical properties, including CS and FS, at intervals of 7, 28, and 90 days. The specimens used were cylinders (150 mm × 300 mm) and prisms (100 mm × 100 mm × 500 mm), tested per ASTM C39 [13] and ASTM C78/C78M-21 [14].

III. RESULTS AND DISCUSSION

i. Flexural Strength

Structural elements like slabs, beams, and columns often experience bending stresses from live and dead loads, making their structural stability and flexural strength (FS) crucial [15]. FS test outcomes for GC blends cured over 7, 28, and 90 days are illustrated in Figure 2, showing a pattern similar to that of compressive strength results. The study confirms that FS improves over time due to hydration reactions [16]. Seven GC blends underwent FS testing up to 90 days, with 7-day FS values for blends R70-G15-C15, R55-G30-C15, R55-G15-C30, R40-G45-C15, R40-G30-C30, R40-G15-C45, and R25-G60-C15 recorded as 1.57 MPa, 1.87 MPa, 2.26 MPa, 2.64 MPa, 2.07 MPa, 2.41 MPa, and 2.31 MPa, respectively, rising to 6.17 MPa, 6.75 MPa, 7.87 MPa, 8.49 MPa, 7.29 MPa, 8.1 MPa, and 7.96 MPa by 90 days. The highest FS was achieved by substituting 45% BR with 45% GGBS and 15% CSD, whereas GGBS and CSD contents over 60% led to FS reduction due to dilution effects in the binding network [17].

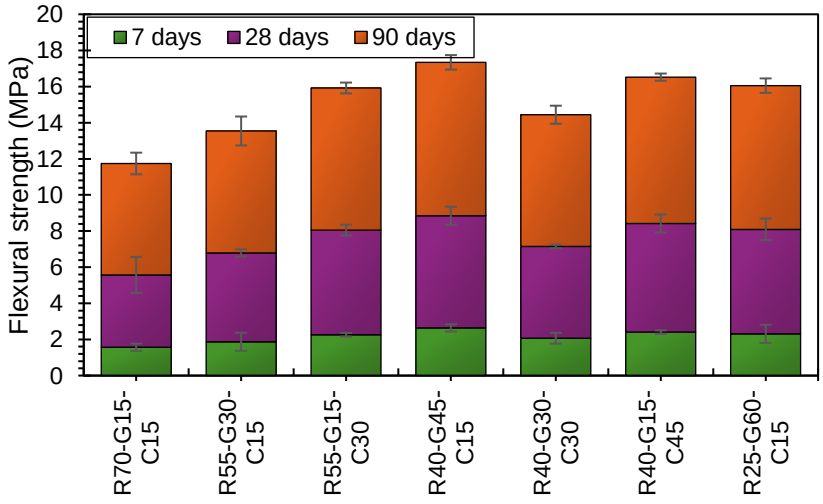

Figure 2. Flexural strength of various GC mixes

ii. Split Tensile Strength

Figure 3 illustrates the change in split tensile strength (STS) of various GC blends over multiple curing periods. At 28 days, the STS values for blends R70-G15-C15, R55-G30-C15, R55-G15-C30, R40-G45-C15, R40-G30-C30, R40-G15-C45, and R25-G60-C15 were 1.98 MPa, 2.34 MPa, 2.54 MPa, 4.57 MPa, 3.83 MPa, 4.14 MPa, and 3.53 MPa, respectively. Using 45% GGBS and 15% CSD produced the highest tensile strength, with increases of 133.33%, 130.81%, and 73.12% at 7, 28, and 90 days, respectively. By 90 days, the STS values had reached 3.2 MPa, 3.6 MPa, 3.92 MPa, 5.54 MPa, 5.05 MPa, 5.29 MPa, and 5.14 MPa [18-20].

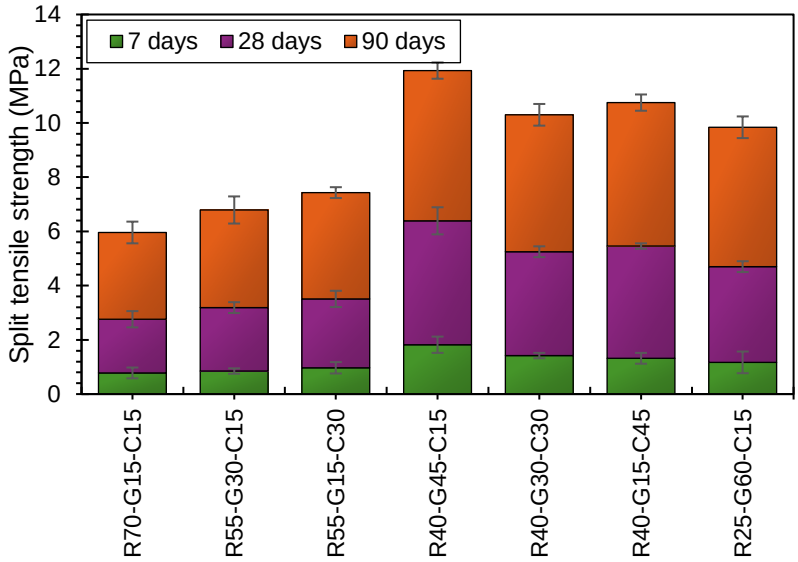

Figure 3. Split tensile strength of various GC mixes

iii. High-Temperature Effect

The GC specimens aged for 28 days were heated to 250°C, 500°C, and 750°C, and the reductions in their mechanical strengths were evaluated in comparison to their strength at 25°C. Figure 4 shows the results of CS, FS, and STS tests on samples after exposure to these elevated temperatures. The strength trend for GC mixes demonstrated that as temperature increased, their mechanical integrity gradually weakened. While mechanical strength did not sharply decline at lower temperatures—in some instances even increasing due to additional geopolymerization and densification—initial signs of strength loss emerged at 250°C, attributed to dehydration and thermal stress [21, 22]. At 500°C, the GC mix's strength typically reduced more due to matrix dehydration and binder breakdown, causing micro-cracks and structural weakening. At 750°C, significant thermal degradation processes, including alumino-silicate bond disruption and potential sintering, led to extensive cracking and further loss of integrity [23]. The general trend showed initial stability or minor gains in strength at lower temperatures, followed by a steady decline at higher temperatures. Among the mixes, R40-G45-C15 showed the least strength reduction. Its CS dropped to 39.57 MPa, 29.61 MPa, and 11.41 MPa from an original 45.27 MPa at 250°C, 500°C, and 750°C, equating to losses of 14.40%, 52.88%, and 296.75%, respectively. Likewise, FS declined from 6.21 MPa to 5.58 MPa, 4.23 MPa, and 2.34 MPa across these temperatures, representing reductions of 11.29%, 46.80%, and 165.38%. Similarly, STS fell to 3.98 MPa, 3.29 MPa, and 1.99 MPa from 4.57 MPa, reflecting losses of 14.82%, 38.90%, and 129.64%. In comparison, R70-G15-C15 exhibited more severe reductions, indicating lower fire resistance with CS losses of 49.68%, 107.53%, and 603.26%; FS losses of 24.61%, 89.57%, and 304.04%; and STS losses of 21.47%, 69.23%, and 241.37% at the same temperatures. The performance of R40-G45-C15 at 750°C underscores its suitability for high-temperature applications due to its superior mechanical resilience.

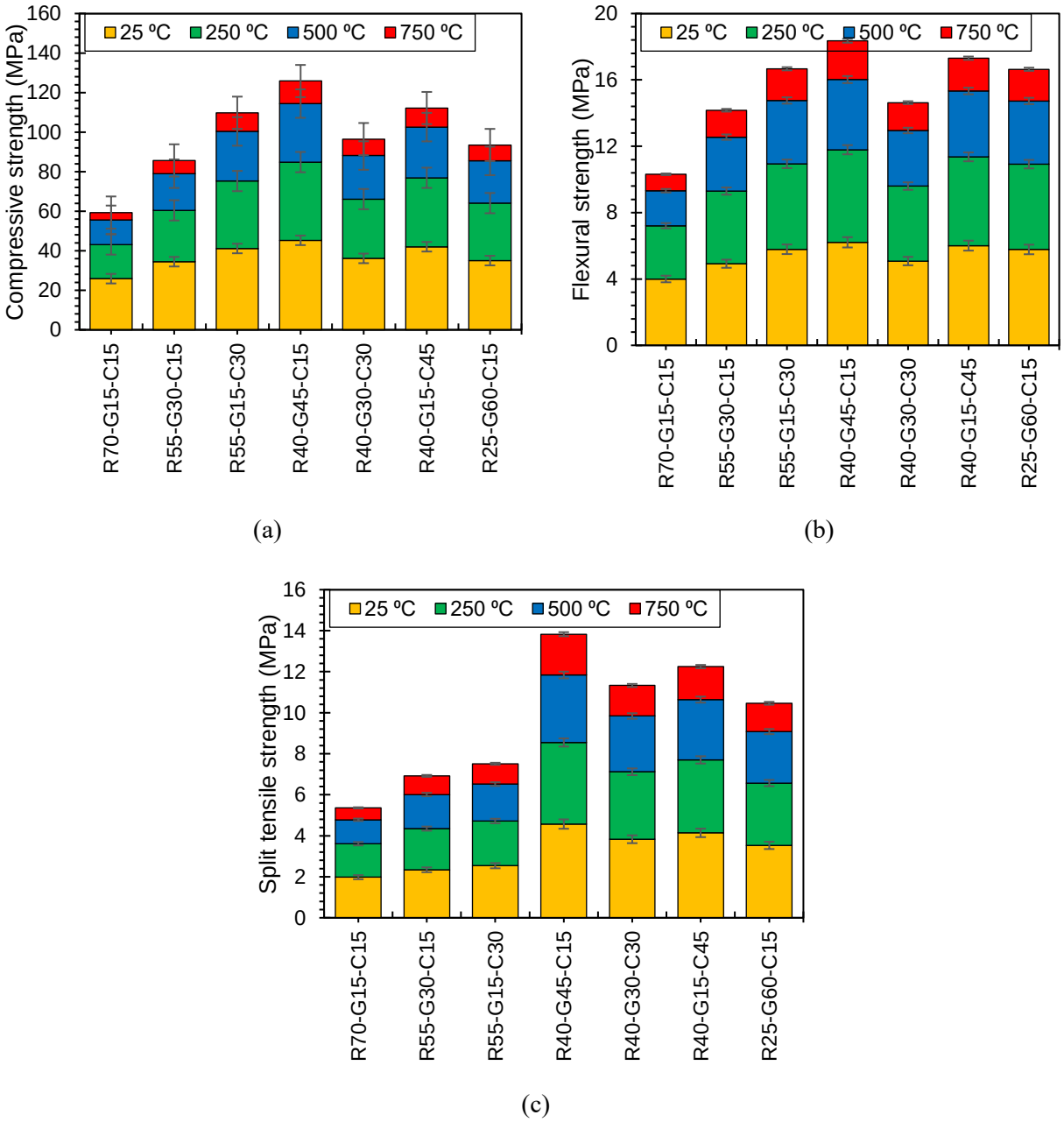

Figure 4. Mechanical strength of GC mixes subjected to high temperatures (a) CS (b) FS, and (c) STS

IV. CONCLUSION

The following key conclusions can be drawn:

- All GC blends demonstrated increased flexural and split tensile strengths over time due to ongoing geopolymerization. Among all mixes, the mix R40-G45-C15 with 40% calcined bauxite residue, 45% GGBS, and 15% CSD achieved the highest flexural, and split tensile strengths, being 53.66% and 112.42% higher than the mix R70-G15-C15 at 28 days, respectively, demonstrating the critical role of curing time and the effectiveness of GGBS and CSD used in the mix.
- The elevated temperatures depicted that at 250°C, 500°C, and 750°C, the blend R40-G45-C15 showed the best results for the compressive strength, which decreased from 45.27 MPa to 39.57 MPa, 29.61 MPa, and 11.41 MPa, respectively. The flexural strength decreased from 6.21 MPa to 5.58 MPa, 4.23 MPa, and 2.34 MPa, respectively, and the splitting tensile strength decreased from 4.57 MPa to 3.98 MPa, 3.29 MPa, and 1.99 MPa, respectively.

REFERENCES

[1] Adnan, A., et al., Structural Efficiency of Fiber-Reinforced Geopolymer Concrete Confined with CFRP Sheets. Technical Journal, 2024. 3(ICACEE): p. 158-165.

[2] Raza, A., et al., Rapid repair of geopolymer concrete members reinforced with polymer composites: Parametric study and analytical modeling. Engineering Structures, 2024. 299: p. 117143.

[3] Raza, A., et al., Microstructural and Thermal Characterization of Polyethylene Fiber-Reinforced Geopolymer Composites. Journal of Building Engineering, 2024: p. 109904.

[4] Raza, A., et al., Mechanical, durability and microstructural characterization of cost-effective polyethylene fiber-reinforced geopolymer concrete. Construction and Building Materials, 2024. 432: p. 136661.

[5] Raza, A., et al., A Comprehensive Review on Material Characterization and Thermal Properties of Geopolymers: Potential of Various Fibers. Case Studies in Construction Materials, 2024: p. e03519.

[6] Yang, Z., et al., Preparation of a geopolymer from red mud slurry and class F fly ash and its behavior at elevated temperatures. Construction and Building Materials, 2019. 221: p. 308-317.

[7] Xue, C., et al., Comparisons of alkali-activated binder concrete (ABC) with OPC concrete-A review. Cement and Concrete Composites, 2023. 135: p. 104851.

[8] *Fawer, M., M. Concannon, and W. Rieber, Life cycle inventories for the production of sodium silicates. The International Journal of Life Cycle Assessment, 1999. 4: p. 207-212.*

[9] Fernando, S., et al., Life cycle assessment and cost analysis of fly ash–rice husk ash blended alkali-activated concrete. Journal of environmental management, 2021. 295: p. 113140.

[10] Ye, N., et al., Transformations of Na, Al, Si and Fe species in red mud during synthesis of one-part geopolymers. Cement and concrete research, 2017. 101: p. 123-130.

[11] Hu, Y., et al., Role of Fe species in geopolymer synthesized from alkali-thermal pretreated Fe-rich Bayer red mud. Construction and Building Materials, 2019. 200: p. 398-407.

[12] ASTM/C143, Standard Test Method for Slump of Hydraulic Cement Concrete, ASTM International, West Conshohocken, PA, 2005.

[13] ASTM C39 / C39M-18. Standard Test Method for Compressive Strength of Cylindrical Concrete Specimens, ASTM International, West Conshohocken, PA 2018.

[14] C78M-21, A.C., Standard Test Method for Flexural Strength of Concrete (Using Simple Beam with Third-Point Loading), ASTM International, West Conshohocken, PA. 2021.

[15] Badkul, A., et al., A comprehensive study on the performance of alkali activated fly ash/GGBFS geopolymer concrete pavement. Road Materials and Pavement Design, 2022. 23(8): p. 1815-1835.

[16] Verma, M. and N. Dev, Sodium hydroxide effect on the mechanical properties of flyash-slag based geopolymer concrete. Structural Concrete, 2021. 22: p. E368-E379.

[17] Hertel, T. and Y. Pontikes, Geopolymers, inorganic polymers, alkali-activated materials and hybrid binders from bauxite residue (red mud)–Putting things in perspective. Journal of Cleaner Production, 2020. 258: p. 120610.

[18] Topark-Ngarm, P., P. Chindaprasirt, and V. Sata, Setting time, strength, and bond of high-calcium fly ash geopolymer concrete. Journal of materials in civil engineering, 2015. 27(7): p. 04014198.

[19] Hua, S., K. Wang, and X. Yao, Developing high performance phosphogypsum-based cementitious materials for oil-well cementing through a step-by-step optimization method. Cement and Concrete Composites, 2016. 72: p. 299-308.

[20] Phoo-ngernkham, T., et al., The effect of adding nano-SiO2 and nano-Al2O3 on properties of high calcium fly ash geopolymer cured at ambient temperature. Materials & Design, 2014. 55: p. 58-65.

[21] Zhang, H.Y., et al., Thermal behavior and mechanical properties of geopolymer mortar after exposure to elevated temperatures. Construction and Building Materials, 2016. 109: p. 17-24.

[22] Kantarci, F., İ. Türkmen, and E. Ekinci, Improving elevated temperature performance of geopolymer concrete utilizing nano-silica, micro-silica and styrene-butadiene latex. Construction and Building Materials, 2021. 286: p. 122980.

[23] Poon, C.-S., et al., Performance of metakaolin concrete at elevated temperatures. Cement and concrete composites, 2003. 25(1): p. 83-89